

## Wnt signaling reduces nuclear acetyl-coA levels to suppress gene expression during osteoblast differentiation

Courtney M. Karner<sup>1,5</sup>, Emel Esen<sup>1,2</sup>, Jiakun Chen<sup>2</sup>, Fong-Fu Hsu<sup>4</sup>, John Turk<sup>4</sup> and Fanxin Long<sup>1,2,3,4,6</sup>

<sup>1</sup> Department of Orthopaedic Surgery, <sup>2</sup> Division of Biology and Biomedical Sciences, <sup>3</sup> Department of Developmental Biology, <sup>4</sup> Department of Medicine, Washington University School of Medicine, Saint Louis, MO 63131

<sup>5</sup> Current Address: Department of Orthopaedic Surgery, Duke University School of Medicine, Durham, NC 27710

<sup>6</sup> Correspondence: [flong@wustl.edu](mailto:flong@wustl.edu)

Running title: Wnt suppresses histone acetylation

**Keywords:** Wnt, osteoblast differentiation, adipogenesis, glucose metabolism, epigenetic regulation, histone acetylation

### ABSTRACT

Developmental signals in metazoans play critical roles in inducing cell differentiation from multipotent progenitors. The existing paradigm posits that the signals operate directly through their downstream transcription factors to activate expression of cell-type-specific genes, which are the hallmark of cell identity. We have investigated the mechanism through which WNT signaling induces osteoblast differentiation in an osteoblast-adipocyte bipotent progenitor cell line. Unexpectedly, WNT3A acutely suppresses the expression of a large number of genes while inducing osteoblast differentiation. The suppressed genes include *Pparg* and *Cebpa* which encode adipocyte-specifying transcription factors, and suppression of which is sufficient to induce osteoblast differentiation. The large-scale gene suppression induced by WNT3A corresponds to a global decrease in histone acetylation, an epigenetic modification that is associated with gene activation. Mechanistically, WNT3A does not alter histone acetyltransferase or deacetylase activities, but rather decreases the level of acetyl-CoA in the nucleus. The Wnt-induced decrease in histone acetylation is independent of  $\beta$ -catenin signaling but rather correlates with suppression of glucose metabolism in the tricarboxylic acid (TCA) cycle. Functionally, preventing histone deacetylation by increasing nucleocytoplasmic acetyl-CoA levels impairs WNT3A-induced osteoblast differentiation. Thus, WNT signaling induces osteoblast differentiation in part through

histone deacetylation and epigenetic suppression of an alternative cell fate.

### INTRODUCTION

A major challenge in modern biology is to understand the mechanism of cellular differentiation in metazoans. Although sharing the same genes, the diverse cell types of a given organism each exhibit a unique profile of gene expression. Gene expression in turn is regulated by the local chromatin milieu at each gene locus. At the molecular level, this milieu reflects epigenetic modifications of both DNA (e.g., methylation) and the associated proteins such as histones (1). Among histone modifications, acetylation and methylation have been most extensively studied. Whereas histone acetylation is often associated with active gene expression, the roles of histone methylation are more complex depending on the position of the lysine residue being modified (2,3). Thus, epigenetic modifications of the chromatin are at the core of cell differentiation. Although it is known that a small number of developmental signals are chiefly responsible for cell differentiation, it is not well understood how these signals confer the epigenetic modifications necessary for cell-type-specific gene expression. Studies to date have focused mostly on the direct downstream transcription factors that engage specific genomic loci and recruit chromatin-modifying enzymes. However, it is becoming increasingly clear that various metabolic intermediates, such as NAD<sup>+</sup>, acetyl-coA and  $\alpha$ -ketoglutarate, can also influence the epigenetic

modifications of the chromatin milieu (4-6). Whether or not developmental signals may exert epigenetic regulation through intermediate metabolites has not been explored.

WNT signaling is a critical regulator of cell differentiation in metazoans both during embryogenesis and in postnatal tissue homeostasis<sup>1,2</sup>. WNT proteins are secreted glycoproteins that activate multiple intracellular signaling cascades. In the most well characterized pathway, WNT stabilizes  $\beta$ -catenin, which enters the nucleus and interacts with the Lef/Tcf family of transcription factors to activate downstream target genes. In addition, WNT proteins can also activate the Rho family of small GTPases, the  $\text{Ca}^{2+}$  pathway, PKC $\delta$ , mTORC1 and mTORC2 (7-13). Through the various effectors, Wnt signaling has been recently shown to regulate cellular metabolism in both normal and cancerous cells (14-17). WNT signaling has been shown to regulate chromatin modifications through  $\beta$ -catenin, which forms complexes with a number of chromatin-modifying enzymes including histone acetyltransferases (HAT) TIP60 and CBP/p300, the H3K4 histone methyltransferase MLL1/MLL2 complex, and the H3K79 histone methyltransferase Dot1-containing complex (18-21). However, potential epigenetic regulation by WNT through  $\beta$ -catenin-independent mechanisms is largely unexplored.

Wnt signaling has emerged as an important mechanism regulating bone formation in mammals (22). In the mouse embryo, deletion of  $\beta$ -catenin, or both LRP5 and LRP6, in the skeletogenic progenitors abolishes osteoblast differentiation, indicating that WNT signaling through  $\beta$ -catenin is critical for embryonic osteoblastogenesis (23-27). In postnatal life, loss- and gain-of-function mutations in LRP5 cause low and high bone mass syndromes, respectively, in humans (28-30). Moreover, deficiency in SOST, a secreted inhibitor that prevents the binding of WNT to LRP5 or LRP6, results in high bone mass in human patients (31,32). In the mouse, deletion of LRP5 causes osteopenia (33,34), whereas loss of SOST increases bone mass (35). The mechanism through which WNT signaling stimulates osteoblast differentiation, however, remains incompletely understood.

Here we present evidence that WNT signaling induces osteoblast differentiation in part

through rapid epigenetic suppression of genes responsible for alternative cell fates. Specifically, WNT3A acutely reduces nuclear acetyl-coA, the necessary substrate for histone acetyltransferases, resulting in a global decrease in histone acetylation. These data reveal a novel mechanism by which WNT signaling suppresses alternative cell fates through modulation of acetyl-coA levels in the cell.

## EXPERIMENTAL PROCEDURES

### Cell culture

ST2 cells were cultured in  $\alpha$ -MEM (Gibco) supplemented with 10% FBS (Invitrogen), 5mM glucose and 2mM glutamine. All experiments were carried out at a seeding density of 13,000 cells/cm<sup>2</sup>. Wnt treatments were initiated 24 hours after plating by replacing the medium with  $\alpha$ -MEM supplemented with 50 ng/ml recombinant Wnt3a (R&D) versus vehicle control (0.1% Chaps in PBS), or by replacing the medium with  $\alpha$ -MEM diluted 1:1 with Wnt3a- or L-Cell (L) conditioned media (CM). In the Dkk1 experiment, the cells were pretreated with 500 ng/ml Dkk1 for 1 hr prior to treatment with Wnt3a and Dkk1 for 6 hours. BMP2 treatments were initiated by replacing the medium with  $\alpha$ -MEM supplemented with either 300 ng/ml recombinant BMP2 (R&D) or vehicle control (0.1% HCl). In indicated experiments, growth media was supplemented 10 ng/ml trichostatin A or 20 mM sodium acetate. For Wnt3a- or BMP2-induced mineralization, cells were treated with Wnt3a or BMP2 with or without the other reagents as indicated for 72 hours, and then switched to mineralization media ( $\alpha$ -MEM supplemented with 50 mg/ml ascorbic acid (Sigma) and 10 mM  $\beta$ -glycerophosphate (Sigma) for 6 days with a change of media every 48 hours. Mineralization was assayed by von Kossa staining.

### Overexpression of dnTCF4, Wnt7b, Wnt10b or Pdk1

ST2 cells were infected with retroviral vectors expressing either empty vector (IE) or dnTCF4, Wnt7b or Wnt10b for 12 hours followed by a 12 hour recovery. The viruses were constructed as previously described (23). For overexpression of Pdk1, ST2 cells were co-infected with lentiviruses expressing FUW-rtTA

and FUW-tetO-myc-Pdk1-IRES-GFP or the control FUW-tetO-IRES-GFP, and then induced with 100ng/ml doxycycline. Pdk1 protein expression was detected by Western blotting with a specific antibody (Enzo #ADI-KAP-PK112, 1:1000 dilution).

### shRNA or siRNA knockdowns

Lentiviral vectors expressing shRNA against  $\beta$ -catenin and Pparg were obtained from the RNAi core at Washington University School of Medicine. The lentiviral vector pLKOpuro was modified to express shRNAs targeting  $\beta$ -catenin, Pparg, or either LacZ or RFP as negative controls (Table 1). The shRNA-expressing lentiviral vector was co-transfected with plasmids pMD2.g and psPax2 into 293 cells. Viral containing media were collected and filtered. ST2 cells were plated at 13,000 cells/cm<sup>2</sup> and infected for 12 hours, and then recovered for 36 hours in regular media. Acly was knocked down with the siRNA On-Targetplus SMART pool (Dharmacon) as follows. ST2 cells were plated at 4,200 cells/cm<sup>2</sup> and transfected with 25 nM SMARTpool #104112 and 0.25  $\mu$ l DUO transfection reagent (Dharmacon) for 48 hours.

### HDAC and HAT activity assays

HDAC activity was measured in 50  $\mu$ g nuclear extract with the Fluor-de-lys HDAC fluorometric activity assay kit (Enzo Life Sciences, BML-AK500). HAT activity was measured in 50  $\mu$ g nuclear lysate by a colorimetric HAT assay (Abcam, ab65352). Each assay was performed in technical triplicate from three independent experiments.

### RNA isolation and qPCR

Total RNA was isolated from cultured cells using the RNeasy kit with on-column DNase treatment (Qiagen). Reverse transcription was performed using 100ng total RNA with the iScript cDNA synthesis kit (BioRad). Reactions were set up in technical and biological triplicates in a 96 well format on an ABI StepOne Plus, using SYBR green chemistry (SsoAdvanced, BioRad). The PCR conditions were 95°C for 3 min followed by 40 cycles of 95°C for 10s and 60°C for 30s. Gene expression was normalized to 18S rRNA and relative expression was calculated using the 2<sup>-( $\Delta\Delta$ Ct)</sup>

method. Primers were used at 0.1  $\mu$ M, and their sequences are listed in Table 2. PCR efficiency was optimized and melting curve analyses of products were performed to ensure reaction specificity.

### RNA-Seq

Poly-A RNA was isolated from 20  $\mu$ g total RNA using Oligo-dT beads. mRNA was fragmented and reverse transcribed into double stranded cDNA. cDNA was blunt-ended, followed by the addition of “A” base to 3’ end and the ligation of sequencing adapters to the ends. The fragments then underwent PCR amplification for 12 cycles. The resulting libraries were sequenced using the Illumina HiSeq-2000 as single reads extending 42 bases (GTAC, Washington University). The raw data was demultiplexed and aligned to the reference genome (mm9) using TopHat. Both Cufflinks and Partek Genomic Suite were used independently to assemble transcripts and analyze expression. Gene Ontology analysis was performed using the GORILLA platform.

### ChIP-seq

Chromatin and protein complexes from 1.5x10<sup>7</sup> ST2 cells were crosslinked for 10 minutes in 1% formaldehyde and flash frozen. Chromatin was sonicated to an average size of 200-450 bp using a Sonics Vibracell sonicator (model Vcx 500). Chromatin complexes were immunoprecipitated using antibodies that recognized the following histone modifications: H3K9ac (Millipore 17-658) and H3K4me3 (Millipore CS200580). ChIP DNA was purified using the PCR purification kit (Qiagen), blunt ended, had addition of an “A” base to 3’ end, and had sequencing adapters ligated to the ends. The fragments were size selected to 200-500 base pairs, and underwent PCR amplification for 15 cycles. The resulting libraries were sequenced using the Illumina HiSeq-2000 as single reads extending 42 bases. The raw data was demultiplexed and aligned to the reference genome (mm9) using Bowtie. MACS was used for peak calling and generation of Wiggle plots. TSS enrichment, meta-gene analysis and heatmaps were generated using Cistrome.

### Western blotting

ST2 cells were scraped in lysis buffer containing 50 mM Tris (pH 7.4), 15 mM NaCl, 0.5% NP-40, and a protease inhibitor mix (Roche #04693124001). Protein concentration was estimated by the BCA method (Pierce). Protein (20 µg) was resolved on 12% polyacrylamide gel and subjected to immunoblot analysis using the respective antibodies. Prestained dual color protein standards were used as molecular weight markers (Biorad). After protein transfer, the blots were typically cut into multiple strips according to the molecular weight markers so that proteins of different sizes could be detected simultaneously from the same blot. Antibodies against Acly (Cell Signaling #4332, 1:1000 dilution) and  $\beta$ -actin (Cell Signaling #4970, 1:1000 dilution) were used to detect the respective protein levels. The immunoblots were blocked for one hour at room temperature in 5% BSA (TBS, 0.1% Tween) followed by an overnight incubation at 4°C in their respective diluted primary antibody solutions. Membranes were then washed three times using TBS/Tween 0.1% and further incubated with the secondary antibody, HRP goat anti-rabbit (Invitrogen, catalog no. G21234) in 5% BSA (TBS/Tween 0.1%) for 1 hr at room temperature (1:5000). All blots were developed using either the Immuno-Star WesternC Chemiluminescence kit or the Clarity ECL substrate (BioRad). Each experiment was repeated for a minimum of three times with three independently prepared protein samples.

#### **Acid extraction of histones**

For the analysis of histone modifications, histones were acid extracted as described (36). Briefly, cells were trypsinized, washed and incubated in hypotonic lysis buffer (10 mM Tris pH 8, 1 mM KCl, 1.5 mM MgCl<sub>2</sub>, 1 mM DTT) for 30 minutes, and the nuclei were pelleted at 3,000xg for 5 minutes at 4 C. Nuclei were resuspended in 4% H<sub>2</sub>SO<sub>4</sub> and protein was pelleted at 15,000 x g for 10 minutes. Histones were precipitated with 33% trifluoroacetic acid (v/v), washed 2x with acetone, dried and resuspended in DI water. Histones were quantified using the BCA method and confirmed by coomassie staining. Histones (1µg) were resolved on a 15% acrylamide gel and blotted with antibodies that recognized the following modifications: H3K9/14ac (Cell Signaling #9677), acetylated H3

(Millipore 06-599), H3K9ac (Millipore 17-658), H4K12ac (Millipore 07-595), total H3 (Abcam ab1791), H3K9me3 (Millipore 17-625), H3K36me3 (Abcam ab9050), H3K27me3 (Abcam ab6002), H3K79me3 (Abcam ab2621) and H3K79me2 (Abcam ab3594). All primary antibodies were used at 1:1000 dilution. Loading of histones was monitored by coomassie staining and by detection of total H3 levels. Western blot signals were quantified using Image J software. Each experiment was done a minimum of three times with three independently prepared protein samples.

#### **Acetyl-coA extraction**

For the extraction of acetyl CoA, 12 – 15x10<sup>7</sup> cells were trypsinized, washed and incubated in hypotonic lysis buffer for 30 minutes, and the nuclei were pelleted at 3,000xg for 5 minutes at 4 C. Nuclei were resuspended in 10% Trichloroacetic acid (Sigma). 100 ng propionyl CoA (Sigma) standard was added and the nuclei were sonicated at 20% amplitude for 30 seconds and centrifuged at 15,000 x g for 5 minutes at 4 C to precipitate the protein pellet. The nuclear lysate was bound to an HLB Oasis 3cc column, washed and eluted in 600 µl methanol.

#### **Acetyl-coA quantification by mass spectrometry**

HPLC mass spectrometric analysis of acetyl CoA was conducted on a Thermo Finnigan (San Jose, CA) TSQ Vantage triple-stage quadrupole instrument with Thermo Accela UPLC, operated with Xcalibur software. Lipid extracts with propyl-CoA internal standard were injected with a Thermo Accela autosampler and separated with a Thermo BETASIL C18 reversed-phase column (100 x 2.1 mm; 3µ particle size) coupled to the ESI source, where the skimmer was set at ground potential, the electrospray needle was set at 4.0 kV, and temperature of the heated capillary was 300 °C. Tandem mass spectrometry was operated in the negative-ion mode in which precursor-ion scan of m/z 134.1 with a collision energy of 21 V was employed. The tandem quadrupole mass spectra were acquired in the profile mode in the mass range of 390-420 Da with a scan rate of 1 scan/sec for detection of the acyl-CoA as the [M – 2H]<sup>2-</sup> ions. The mass



resolution of the instrument was tuned to 0.6 Da at half peak height.

HPLC separation was carried out with step gradient, in which mobile phase A was 5% acetonitrile in water with 0.1%  $\text{NH}_4\text{OH}$  and mobile phase B was 0.1%  $\text{NH}_4\text{OH}$  in 95% acetonitrile/water. Step gradient elution was performed with an initial condition of 100% A for 4 minutes, and switch to mobile phase B for additional 4 minutes. Column is then re-equilibrated at 100% B for 10 minutes prior to subsequent injections. The flow rate is 50  $\mu\text{L}/\text{min}$  at ambient temperature.

### Nuclear citrate measurement

Nuclear citrate concentration was measured using the citrate fluorometric assay kit (Sigma-Aldrich, MAK057). For the extraction of citrate, nuclei from ST2 cells treated with L- or Wnt3a-conditioned media were resuspended in 0.1mL Citrate Assay Buffer. Insoluble material was removed by centrifugation at 15,000xg for 10 minutes at 4 °C. Nuclear supernatants were concentrated on 10 kD spin columns (Abcam ab93349) at 10,000xg for 20 minutes. 25uL nuclear extract was used for each technical replicate. Citrate concentration was extrapolated from a standard curve and normalized to cell number. Each assay was performed in technical duplicate from six independent experiments.

### CO<sub>2</sub> trap experiments

The procedure is as described previously (37). Briefly, ST2 cells were seeded at  $4 \times 10^5/\text{flask}$ , and cultured in media containing 2  $\mu\text{L}$  of 0.1 mCi/mL  $^{14}\text{C}$ -labeled glucose (total radioactivity 444,000 dpm), with or without Wnt3a (100ng/mL), in the sealed CO<sub>2</sub> trap system for 24 hours before CO<sub>2</sub> was harvested for the measurement of radioactivity. [3,4- $^{14}\text{C}$ ]glucose (cat# ARC 0211A) and [6- $^{14}\text{C}$ ]glucose (cat# ARC 0121B) were from American Radiolabeled Chemicals (St Louis, MO). A parallel experiment was conducted with identical treatments for cell counting. For glucose consumption, an aliquot of the medium was taken for measurements before the injection of  $\text{H}_2\text{SO}_4$ .

## RESULTS

### Wnt3a acutely suppresses gene expression

To investigate how Wnt signaling induces osteoblast differentiation, we applied Wnt3a to ST2 cells, a progenitor cell that possesses both osteogenic and adipogenic potential but undergoes osteoblast differentiation in response to Wnt3a (13,38,39). Wnt3a-induced osteoblast differentiation was confirmed by the time-dependent upregulation of marker genes such as *Alpl*, *Ibsp*, *Bglap* and *Sp7* (Fig. 1A). Interestingly, *Sp7* and *Bglap* were initially suppressed by Wnt3a before being upregulated at the later time points. To gain insights about the early transcriptional response to Wnt3a, we profiled the transcriptome by RNA-seq in these cells after 6 and 24 hours of treatment. For comparison, we conducted similar experiments with BMP2, another potent osteogenic signal for ST2 cells. Unexpectedly, Wnt3a suppressed the mRNA levels of a large number of genes as early as 6 hours of treatment (144 genes with > 2 fold decrease), and the number of suppressed genes surpassed those induced at 24 hours (487 versus 329 genes, with > 2 fold change) (Figure 1B). In contrast, BMP2 altered the expression of much fewer genes at 6 hours, and the number of genes suppressed was considerably lower than those induced at both 6 and 24 hours (Figure 1B). The prominent feature of gene suppression by Wnt3a was unexpected, as gene activation through  $\beta$ -catenin is presumed to be the dominant mode of Wnt3a signaling. We performed gene ontology (GO) analysis of genes suppressed at least 2 fold by Wnt3a using GOrilla (40). This analysis revealed that the suppressed transcripts were significantly enriched for genes involved in “positive regulation of cell differentiation” (GO:0045597,  $p=7.22\text{E}^{-10}$ ) and “positive regulation of transcription, DNA-dependent” (GO:0045893,  $p=1.87\text{E}^{-06}$ ). These genetic cadres include transcription factors known to regulate the differentiation of adipocytes (e.g., *Pparg*, *Cebpa* and *Id2*) and chondrocytes (e.g., *Sox5* and *Sox9*) (See Figure 1C for the RNA-seq alignment for the representative gene *Pparg*). With quantitative PCR, we confirmed that these adipogenic or chondrogenic transcription factors were all suppressed upon 6 hours of Wnt3a treatment (Figure 1D). Like recombinant Wnt3a, virally expressed Wnt10b or Wnt7b, both known to induce osteoblast differentiation, caused similar suppression of those genes (data not shown). Others have also observed the suppressive effect

of Wnt10b on *Pparg* and *Cebpa*, and further demonstrated that knockdown of *Pparg* or *Cebpa* induced spontaneous osteoblast differentiation in ST2 cells (38). We confirmed that *Pparg* knockdown (by ~50%) alone was sufficient to induce the expression of osteoblast markers *Alpl* and *Ibsp*, albeit less efficiently than Wnt3a (Figure 1E). In contrast to Wnt, BMP2 did not suppress *Pparg* or *Cebpa*, nor did it impair adipocyte differentiation in ST2 cells (data not shown). Thus, unlike BMP, Wnt appears to induce osteoblast differentiation in part through suppression of adipogenic transcription factors and the alternative cell fate.

### Wnt3a acutely reduces histone acetylation

To investigate the mechanism of gene suppression by Wnt3a, we first evaluated if  $\beta$ -catenin-mediated transcription was required. Expression of a dominant negative TCF4 (dnTCF4) completely abrogated the induction of  $\beta$ -catenin target genes like *Lef1* by Wnt3a, but had no effect on the suppression of *Pparg* or *Cebpa* at either 6 or 96 hrs of Wnt treatment (Figure 2A, B). Similarly, knockdown of  $\beta$ -catenin had no effect on Wnt3a-dependent suppression (Figure 2C). These results are consistent with the fact that Wnt7b suppressed gene expression even though it did not activate  $\beta$ -catenin-dependent gene transcription in ST2 cells (13). Thus, gene suppression in response to Wnt3a is unlikely to be secondary to gene activation mediated by the  $\beta$ -catenin/Tcf complex.

Because histone acetylation and methylation are associated with gene transcription, we next evaluated the effect of Wnt3a on such modifications of bulk histones. Remarkably, after 6 hours of treatment, Wnt3a reduced the acetylation of histone H3, a modification associated with active gene transcription, and the effect lasted for at least 24 hrs (Figure 3A, B). In contrast, BMP2 did not suppress histone acetylation (Figure 3B). The suppression of histone acetylation by Wnt3a likely required Lrp5/6 signaling as Dkk1, which is known to interfere with the Wnt-Lrp5/6 interaction, notably diminished the effect (Figure 3C). A survey of several histone methylation marks indicated that Wnt3a did not alter the levels of H3K9me3, H3K27me3, H3K4me3 or H3K36me3, although it increased H3K79me3, likely due to the

methyltransferase activity of the  $\beta$ -catenin/Dot complex induced by Wnt signaling as previously reported (19,21). Thus, Wnt signaling acutely reduces histone acetylation, and this event may account for the rapid suppression of gene expression.

We next sought to determine whether the decrease in bulk histone acetylation was reflected by changes on the chromatin. For this, we performed chromatin Immunoprecipitation followed by deep sequencing (ChIP-Seq) using antibodies specific for acetylated H3K9 (H3K9ac) or tri-methylated H3K4 (H3K4me3) to localize these modifications to particular loci on the chromatin. These experiments yielded 4565 genomic loci with decreased H3K9ac compared to only 1461 with increased H3K9ac after 6 hours of Wnt3a stimulation. When examined individually, each autosome contained many more loci with decreased than increased H3K9ac (Figure 3D). In contrast, Wnt3a only minimally affected H3K4me3, with 162 genomic loci showing an increase compared to 141 loci with a decrease. More importantly, all promoter regions (defined as  $\pm 3$  kb flanking the transcription start site – TSS) in the genome on average exhibited a decrease in H3K9ac, but a slight increase in H3K4me3 (Figure 3E). When the promoter regions of all suppressed versus induced genes were analyzed separately, we saw that Wnt3a caused a decrease in H3K9ac in the former, but an increase in H3K4me3 in the later (Figure 3F, G). Finally, 355 of the 4655 loci with decreased H3K9ac were located within 3 kb of a TSS, and showed significant correlation with gene suppression ( $p=2.25 \times 10^{-23}$ , hypergeometric test), as exemplified by *Pparg* and *Sox5* (Fig. 3H,I). Conversely, Wnt3a-induced genes significantly overlapped with genes exhibiting increased H3K9ac in their promoters ( $p=0.00067$ , hypergeometric test). There was no overlap between genes with decreased H3K9ac in the promoter and genes induced, or *vice versa*. Thus, Wnt3a induces a genome-wide reduction in histone acetylation that correlates with broad gene suppression.

### Wnt3a decreases nuclear acetyl-coA and citrate levels

To determine if decreased histone acetylation was required for gene suppression by Wnt signaling. We used trichostatin A (TSA) to

inhibit both class I and II HDACs. TSA greatly increased histone acetylation in ST2 cells regardless of Wnt3a (Figure 4A). Importantly, preventing histone deacetylation with TSA completely abolished Wnt3a-induced suppression of *Pparg* and *Cebpa*, as well as osteoblast differentiation assayed by von Kossa staining (Figure 4B, C).

We next investigated how Wnt3a decreases histone acetylation. We found no change in either histone deacetylase (HDAC) or histone acetyltransferase (HAT) activities in assays with nuclear extracts after 6 hours of Wnt3a treatment (Figure 4D). Therefore, we hypothesized that Wnt3a suppressed histone acetylation by decreasing available acetyl-coA, the substrate for HAT. We directly measured acetyl-coA levels with mass spectrometry in nuclear extracts prepared from ST2 cells. These experiments revealed that Wnt3a reduced nuclear acetyl-coA levels by 25% after 6 hours of treatment (Figure 4E). Thus, Wnt3a suppresses histone acetylation and gene expression likely by reducing nuclear acetyl-coA levels.

Because citrate is the precursor for acetyl-coA, we next examined the potential effect of Wnt3a on citrate levels in the nucleus. For this, we measured citrate levels in nuclear extracts prepared from ST2 cells treated with Wnt3a-conditioned media (Wnt3a-CM) or the control media. Wnt3a-CM reduced nuclear citrate levels by 24% after 6 hours of treatment (Figure 4F). Thus, Wnt3a appears to reduce the nuclear acetyl-coA concentration by suppressing citrate levels.

### Changes in acetyl-coA production affect histone acetylation and gene expression

Our findings so far predict that changing nucleocytoplasmic acetyl-coA levels would affect Wnt3a-induced histone deacetylation and gene suppression. To test this prediction, we treated ST2 cells with supraphysiological levels of acetate, which is converted to acetyl-coA by ACES1 and expected to elevate nucleocytoplasmic acetyl-coA levels (Figure 5A) (5). Acetate by itself slightly increased H3K9ac, and completely reversed the effect of Wnt3a on histone acetylation (Figure 5B). Importantly, acetate not only blunted the suppression of *Pparg* and *Cebpa* by Wnt3a, but also impaired Wnt3a-induced osteoblast differentiation as assayed by

both gene expression and von Kossa staining (Figure 5C-E). We next used siRNA to knock down ATP citrate lyase (*Acly*), the principle enzyme responsible for generating nucleocytoplasmic acetyl-coA from citrate in mammalian cells (Figure 5A) (5). *Acly* knockdown, similar to Wnt3a, markedly decreased H3K9ac levels and suppressed *Pparg* and *Cebpa* expression, but Wnt3a and *Acly* knockdown did not have an additive effect on gene suppression (Figure 5F, G). These results further support the conclusion that Wnt3a suppresses histone acetylation by reducing acetyl-coA levels.

### Wnt3a suppresses glucose entry to TCA cycle to reduce histone acetylation

Glucose oxidation in the TCA cycle is a primary source of citrate for acetyl-coA production, and we have previously shown that Wnt signaling stimulates glucose consumption and lactate production from glucose (5,41). To examine directly the effect of Wnt on glucose oxidation through the TCA cycle, we used a CO<sub>2</sub> trapping method to capture radioactive <sup>14</sup>CO<sub>2</sub> produced from glucose labeled with <sup>14</sup>C at specific positions. In this method, [3,4-<sup>14</sup>C<sub>2</sub>]glucose produces <sup>14</sup>CO<sub>2</sub> upon entry into the TCA cycle via conversion of pyruvate into acetyl-coA and <sup>14</sup>CO<sub>2</sub> (Figure 6A). On the other hand, [6-<sup>14</sup>C]glucose produces <sup>14</sup>CO<sub>2</sub> during the conversion of citrate to α-ketoglutarate after completion of the first round of the TCA cycle (Figure 6B). Despite a greater amount of total glucose consumption, the cells treated with Wnt3a released significantly less <sup>14</sup>CO<sub>2</sub> from [3,4-<sup>14</sup>C<sub>2</sub>]glucose than the control (Figure 6C). Upon normalized to glucose consumption, the percentage of glucose entering the TCA cycle was reduced by nearly 50% by Wnt3a over the control (Figure 6D). On the other hand, the amount of glucose that completes the TCA cycle, as measured by <sup>14</sup>CO<sub>2</sub> radioactivity released from [6-<sup>14</sup>C]glucose, was not affected by Wnt3a (Figure 6E, F). Thus, Wnt signaling reduces the amount of glucose entering the TCA cycle, and this may be responsible for the decrease of citrate and acetyl-CoA levels in the nucleus.

Our data predict that reducing glucose entry into the TCA cycle should mimic the effect of Wnt3a on histone acetylation. As a proof of principle, withdrawal of glucose from the culture media for 12 hours markedly decreased histone

acetylation in ST2 cells (Figure 7A). We next tested whether preventing glucose metabolism into the TCA cycle was sufficient to decrease histone acetylation in the absence of Wnt signaling. Specifically, we overexpressed pyruvate dehydrogenase kinase 1 (Pdk1), which phosphorylates and inhibits pyruvate dehydrogenase thus preventing pyruvate oxidation and entry into the TCA cycle (Figure 7B). Pdk1 overexpression not only reduced histone acetylation by 47%, but also suppressed gene expression of *Pparg* and *Cebpa* in ST2 cells (Figure 7C, D). Thus, Wnt signaling suppresses histone acetylation likely through reprogramming of glucose metabolism.

## DISCUSSION

We have provided evidence that WNT signaling induces osteoblast differentiation in part through epigenetic suppression of gene expression. The data support the mechanism that Wnt3a acutely reprograms glucose metabolism to reduce the nuclear level of citrate and acetyl-coA, resulting in a decrease in histone acetylation independent of  $\beta$ -catenin. The current study expands our understanding about how WNT regulates gene expression.

The study provides a mechanistic link between reduced TCA metabolism of glucose and the early phase of osteoblast differentiation in response to Wnt. Our finding is reminiscent of a recent report that decreased glycolysis reduces acetyl-coA and histone acetylation during early differentiation of embryonic stem cells (42). Thus, a glycolytic switch appears to trigger cellular differentiation in multiple settings.

Our study reveals that Wnt signaling induces osteoblast differentiation in part through epigenetic suppression of transcription factors specifying the alternative fate of adipocyte. In contrast, BMP2 does not utilize the same mechanism, but rather induces the expression of Sp7, an osteogenic transcription factor. Thus, in ST2 cells, WNT and BMP induce osteoblast differentiation through apparently different mechanisms. It should be noted that  $\beta$ -catenin is also necessary for Wnt3a-induced osteoblast

differentiation in ST2 cells as knockdown of  $\beta$ -catenin essentially abolished the induction of *Alpl*. Thus, WNT signaling induces osteoblast differentiation both by gene activation via  $\beta$ -catenin, and by gene suppression through acetyl-coA-mediated epigenetic regulation.

Our findings may have broad implications for understanding epigenetic regulations of gene expression. The prevailing view holds that epigenetic changes require *de novo* binding of transcription factors to specific DNA sequences which subsequently recruit chromatin-modifying enzymes. Our results however, indicate that developmental signals can act through intermediate metabolites to alter chromatin modifications and gene expression. The acute response in the level of histone acetylation likely reflects the dynamic nature of acetylation versus deacetylation on the genomic loci already occupied by the respective enzymes. Although our in vitro assays did not detect any change in total Hdac or Hat activity in nuclear extracts in response to Wnt3a, the results do not exclude the possibility that the enzymatic activity might be altered in vivo. Indeed, a recent study has linked decreased intracellular pH with global histone deacetylation (43). Considering our previous finding that Wnt signaling stimulates lactate production from glucose, it is conceivable that a lower intracellular pH could result and also contribute to histone deacetylation (41). Although previous studies have shown that chromatin acetylation decreased with differentiation of embryonic stem cells, they did not demonstrate a causal relationship between deacetylation and differentiation (44). Interestingly, Acly knockdown induces differentiation in C2C12 myoblasts, but does not affect differentiation of 3T3L1 preadipocytes even though it prevents lipid accumulation, indicating that modulation of acetyl-CoA levels likely has a context dependent role during differentiation (5,45). Finally, the present study raises the possibility that other substrates or co-factors for chromatin-modifying enzymes may also respond to physiological signals in a biologically meaningful way to affect gene expression.



**Acknowledgements**

We thank Paul Cliften (Washington University School of Medicine) for help with MACS and bioinformatics.

**Conflict of interest:** The authors declare that they have no conflicts of interest with the contents of this article.

**Author contributions:** CMK, EE, JC conducted most of the experiments, FH and JT performed mass spectrometric measurements of acetyl-coA, FL conceived the idea for the project, CMK and FL analyzed the data and wrote the paper.

## REFERENCES

1. Goldberg, A. D., Allis, C. D., and Bernstein, E. (2007) Epigenetics: a landscape takes shape. *Cell* **128**, 635-638
2. Jenuwein, T., and Allis, C. D. (2001) Translating the histone code. *Science* **293**, 1074-1080
3. Kouzarides, T. (2007) Chromatin modifications and their function. *Cell* **128**, 693-705
4. Guarente, L. (2000) Sir2 links chromatin silencing, metabolism, and aging. *Genes & development* **14**, 1021-1026
5. Wellen, K. E., Hatzivassiliou, G., Sachdeva, U. M., Bui, T. V., Cross, J. R., and Thompson, C. B. (2009) ATP-citrate lyase links cellular metabolism to histone acetylation. *Science* **324**, 1076-1080
6. Tsukada, Y., Fang, J., Erdjument-Bromage, H., Warren, M. E., Borchers, C. H., Tempst, P., and Zhang, Y. (2006) Histone demethylation by a family of JmjC domain-containing proteins. *Nature* **439**, 811-816
7. Inoki, K., Ouyang, H., Zhu, T., Lindvall, C., Wang, Y., Zhang, X., Yang, Q., Bennett, C., Harada, Y., Stankunas, K., Wang, C. Y., He, X., MacDougald, O. A., You, M., Williams, B. O., and Guan, K. L. (2006) TSC2 integrates Wnt and energy signals via a coordinated phosphorylation by AMPK and GSK3 to regulate cell growth. *Cell* **126**, 955-968
8. Habas, R., Dawid, I. B., and He, X. (2003) Coactivation of Rac and Rho by Wnt/Frizzled signaling is required for vertebrate gastrulation. *Genes Dev* **17**, 295-309
9. Habas, R., Kato, Y., and He, X. (2001) Wnt/Frizzled activation of Rho regulates vertebrate gastrulation and requires a novel Formin homology protein Daam1. *Cell* **107**, 843-854
10. Wu, X., Tu, X., Joeng, K. S., Hilton, M. J., Williams, D. A., and Long, F. (2008) Rac1 activation controls nuclear localization of beta-catenin during canonical Wnt signaling. *Cell* **133**, 340-353
11. Kuhl, M., Sheldahl, L. C., Park, M., Miller, J. R., and Moon, R. T. (2000) The Wnt/Ca<sup>2+</sup> pathway: a new vertebrate Wnt signaling pathway takes shape. *Trends Genet* **16**, 279-283
12. Kinoshita, N., Iioka, H., Miyakoshi, A., and Ueno, N. (2003) PKC delta is essential for Dishevelled function in a noncanonical Wnt pathway that regulates *Xenopus* convergent extension movements. *Genes Dev* **17**, 1663-1676
13. Tu, X., Joeng, K. S., Nakayama, K. I., Nakayama, K., Rajagopal, J., Carroll, T. J., McMahon, A. P., and Long, F. (2007) Noncanonical Wnt Signaling through G Protein-Linked PKCdelta Activation Promotes Bone Formation. *Dev Cell* **12**, 113-127
14. Yoon, J. C., Ng, A., Kim, B. H., Bianco, A., Xavier, R. J., and Elledge, S. J. (2010) Wnt signaling regulates mitochondrial physiology and insulin sensitivity. *Genes & development* **24**, 1507-1518

15. Frey, J. L., Li, Z., Ellis, J. M., Zhang, Q., Farber, C. R., Aja, S., Wolfgang, M. J., Clemens, T. L., and Riddle, R. C. (2015) Wnt-Lrp5 signaling regulates fatty acid metabolism in the osteoblast. *Molecular and cellular biology* **35**, 1979-1991
16. Pate, K. T., Stringari, C., Sprowl-Tanio, S., Wang, K., TeSlaa, T., Hoverter, N. P., McQuade, M. M., Garner, C., Digman, M. A., Teitell, M. A., Edwards, R. A., Gratton, E., and Waterman, M. L. (2014) Wnt signaling directs a metabolic program of glycolysis and angiogenesis in colon cancer. *The EMBO journal* **33**, 1454-1473
17. Karner, C. M., Esen, E., Okunade, A. L., Patterson, B. W., and Long, F. (2015) Increased glutamine catabolism mediates bone anabolism in response to WNT signaling. *The Journal of clinical investigation* **125**, 551-562
18. Hecht, A., Vleminckx, K., Stemmler, M. P., van Roy, F., and Kemler, R. (2000) The p300/CBP acetyltransferases function as transcriptional coactivators of beta-catenin in vertebrates. *The EMBO journal* **19**, 1839-1850
19. Mohan, M., Herz, H. M., Takahashi, Y. H., Lin, C., Lai, K. C., Zhang, Y., Washburn, M. P., Florens, L., and Shilatifard, A. (2010) Linking H3K79 trimethylation to Wnt signaling through a novel Dot1-containing complex (DotCom). *Genes & development* **24**, 574-589
20. Sierra, J., Yoshida, T., Joazeiro, C. A., and Jones, K. A. (2006) The APC tumor suppressor counteracts beta-catenin activation and H3K4 methylation at Wnt target genes. *Genes & development* **20**, 586-600
21. Mahmoudi, T., Boj, S. F., Hatzis, P., Li, V. S., Taouatas, N., Vries, R. G., Teunissen, H., Begthel, H., Korving, J., Mohammed, S., Heck, A. J., and Clevers, H. (2010) The leukemia-associated Mllt10/Af10-Dot1l are Tcf4/beta-catenin coactivators essential for intestinal homeostasis. *PLoS biology* **8**, e1000539
22. Long, F. (2012) Building strong bones: molecular regulation of the osteoblast lineage. *Nature reviews. Molecular cell biology* **13**, 27-38
23. Hu, H., Hilton, M. J., Tu, X., Yu, K., Ornitz, D. M., and Long, F. (2005) Sequential roles of Hedgehog and Wnt signaling in osteoblast development. *Development* **132**, 49-60
24. Day, T. F., Guo, X., Garrett-Beal, L., and Yang, Y. (2005) Wnt/beta-catenin signaling in mesenchymal progenitors controls osteoblast and chondrocyte differentiation during vertebrate skeletogenesis. *Dev Cell* **8**, 739-750
25. Hill, T. P., Spater, D., Taketo, M. M., Birchmeier, W., and Hartmann, C. (2005) Canonical Wnt/beta-catenin signaling prevents osteoblasts from differentiating into chondrocytes. *Dev Cell* **8**, 727-738
26. Rodda, S. J., and McMahon, A. P. (2006) Distinct roles for Hedgehog and canonical Wnt signaling in specification, differentiation and maintenance of osteoblast progenitors. *Development* **133**, 3231-3244
27. Joeng, K. S., Schumacher, C. A., Zylstra-Diegel, C. R., Long, F., and Williams, B. O. (2011) Lrp5 and Lrp6 redundantly control skeletal development in the mouse embryo. *Developmental biology* **359**, 222-229
28. Gong, Y., Slee, R. B., Fukai, N., Rawadi, G., Roman-Roman, S., Reginato, A. M., Wang, H., Cundy, T., Glorieux, F. H., Lev, D., Zacharin, M., Oexle, K., Marcelino,

- J., Suwairi, W., Heeger, S., Sabatakos, G., Apte, S., Adkins, W. N., Allgrove, J., Arslan-Kirchner, M., Batch, J. A., Beighton, P., Black, G. C., Boles, R. G., Boon, L. M., Borrone, C., Brunner, H. G., Carle, G. F., Dallapiccola, B., De Paepe, A., Floege, B., Halfhide, M. L., Hall, B., Hennekam, R. C., Hirose, T., Jans, A., Juppner, H., Kim, C. A., Keppler-Noreuil, K., Kohlschuetter, A., LaCombe, D., Lambert, M., Lemyre, E., Letteboer, T., Peltonen, L., Ramesar, R. S., Romanengo, M., Somer, H., Steichen-Gersdorf, E., Steinmann, B., Sullivan, B., Superti-Furga, A., Swoboda, W., van den Boogaard, M. J., Van Hul, W., Vikkula, M., Votruba, M., Zabel, B., Garcia, T., Baron, R., Olsen, B. R., and Warman, M. L. (2001) LDL receptor-related protein 5 (LRP5) affects bone accrual and eye development. *Cell* **107**, 513-523
29. Little, R. D., Carulli, J. P., Del Mastro, R. G., Dupuis, J., Osborne, M., Folz, C., Manning, S. P., Swain, P. M., Zhao, S. C., Eustace, B., Lappe, M. M., Spitzer, L., Zweier, S., Braunschweiger, K., Benchekroun, Y., Hu, X., Adair, R., Chee, L., FitzGerald, M. G., Tulig, C., Caruso, A., Tzellas, N., Bawa, A., Franklin, B., McGuire, S., Nogues, X., Gong, G., Allen, K. M., Anisowicz, A., Morales, A. J., Lomedico, P. T., Recker, S. M., Van Eerdewegh, P., Recker, R. R., and Johnson, M. L. (2002) A mutation in the LDL receptor-related protein 5 gene results in the autosomal dominant high-bone-mass trait. *Am J Hum Genet* **70**, 11-19
  30. Boyden, L. M., Mao, J., Belsky, J., Mitzner, L., Farhi, A., Mitnick, M. A., Wu, D., Insogna, K., and Lifton, R. P. (2002) High bone density due to a mutation in LDL-receptor-related protein 5. *N Engl J Med* **346**, 1513-1521
  31. Balemans, W., Patel, N., Ebeling, M., Van Hul, E., Wuyts, W., Lacza, C., Dioszegi, M., Dikkers, F. G., Hildering, P., Willems, P. J., Verheij, J. B., Lindpaintner, K., Vickery, B., Foernzler, D., and Van Hul, W. (2002) Identification of a 52 kb deletion downstream of the SOST gene in patients with van Buchem disease. *J Med Genet* **39**, 91-97
  32. Balemans, W., Ebeling, M., Patel, N., Van Hul, E., Olson, P., Dioszegi, M., Lacza, C., Wuyts, W., Van Den Ende, J., Willems, P., Paes-Alves, A. F., Hill, S., Bueno, M., Ramos, F. J., Tacconi, P., Dikkers, F. G., Stratakis, C., Lindpaintner, K., Vickery, B., Foernzler, D., and Van Hul, W. (2001) Increased bone density in sclerosteosis is due to the deficiency of a novel secreted protein (SOST). *Hum Mol Genet* **10**, 537-543
  33. Kato, M., Patel, M. S., Levasseur, R., Lobov, I., Chang, B. H., Glass, D. A., 2nd, Hartmann, C., Li, L., Hwang, T. H., Brayton, C. F., Lang, R. A., Karsenty, G., and Chan, L. (2002) Cbfa1-independent decrease in osteoblast proliferation, osteopenia, and persistent embryonic eye vascularization in mice deficient in Lrp5, a Wnt coreceptor. *J Cell Biol* **157**, 303-314
  34. Cui, Y., Niziolek, P. J., Macdonald, B. T., Zylstra, C. R., Alenina, N., Robinson, D. R., Zhong, Z., Matthes, S., Jacobsen, C. M., Conlon, R. A., Brommage, R., Liu, Q., Mseeh, F., Powell, D. R., Yang, Q. M., Zambrowicz, B., Gerrits, H., Gossen, J. A., He, X., Bader, M., Williams, B. O., Warman, M. L., and Robling, A. G. (2011) Lrp5 functions in bone to regulate bone mass. *Nature medicine* **17**, 684-691



35. Li, X., Ominsky, M. S., Niu, Q. T., Sun, N., Daugherty, B., D'Agostin, D., Kurahara, C., Gao, Y., Cao, J., Gong, J., Asuncion, F., Barrero, M., Warmington, K., Dwyer, D., Stolina, M., Morony, S., Sarosi, I., Kostenuik, P. J., Lacey, D. L., Simonet, W. S., Ke, H. Z., and Paszty, C. (2008) Targeted deletion of the sclerostin gene in mice results in increased bone formation and bone strength. *Journal of bone and mineral research : the official journal of the American Society for Bone and Mineral Research* **23**, 860-869
36. Shechter, D., Dormann, H. L., Allis, C. D., and Hake, S. B. (2007) Extraction, purification and analysis of histones. *Nat Protoc* **2**, 1445-1457
37. Esen, E., Lee, S. Y., Wice, B. M., and Long, F. (2015) PTH Promotes Bone Anabolism by Stimulating Aerobic Glycolysis Via IGF Signaling. *Journal of bone and mineral research : the official journal of the American Society for Bone and Mineral Research*
38. Kang, S., Bennett, C. N., Gerin, I., Rapp, L. A., Hankenson, K. D., and Macdougald, O. A. (2007) Wnt signaling stimulates osteoblastogenesis of mesenchymal precursors by suppressing CCAAT/enhancer-binding protein alpha and peroxisome proliferator-activated receptor gamma. *The Journal of biological chemistry* **282**, 14515-14524
39. Ogawa, M., Nishikawa, S., Ikuta, K., Yamamura, F., Naito, M., and Takahashi, K. (1988) B cell ontogeny in murine embryo studied by a culture system with the monolayer of a stromal cell clone, ST2: B cell progenitor develops first in the embryonal body rather than in the yolk sac. *Embo J* **7**, 1337-1343
40. Eden, E., Navon, R., Steinfeld, I., Lipson, D., and Yakhini, Z. (2009) GOrilla: a tool for discovery and visualization of enriched GO terms in ranked gene lists. *BMC Bioinformatics* **10**, 48
41. Esen, E., Chen, J., Karner, C. M., Okunade, A. L., Patterson, B. W., and Long, F. (2013) WNT-LRP5 signaling induces Warburg effect through mTORC2 activation during osteoblast differentiation. *Cell metabolism* **17**, 745-755
42. Moussaieff, A., Rouleau, M., Kitsberg, D., Cohen, M., Levy, G., Barasch, D., Nemirovski, A., Shen-Orr, S., Laevsky, I., Amit, M., Bomze, D., Elena-Herrmann, B., Scherf, T., Nissim-Rafinia, M., Kempa, S., Itskovitz-Eldor, J., Meshorer, E., Aberdam, D., and Nahmias, Y. (2015) Glycolysis-mediated changes in acetyl-CoA and histone acetylation control the early differentiation of embryonic stem cells. *Cell metabolism* **21**, 392-402
43. McBrian, M. A., Behbahan, I. S., Ferrari, R., Su, T., Huang, T. W., Li, K., Hong, C. S., Christofk, H. R., Vogelauer, M., Seligson, D. B., and Kurdistani, S. K. (2013) Histone acetylation regulates intracellular pH. *Molecular cell* **49**, 310-321
44. Meshorer, E., Yellajoshula, D., George, E., Scambler, P. J., Brown, D. T., and Misteli, T. (2006) Hyperdynamic plasticity of chromatin proteins in pluripotent embryonic stem cells. *Developmental cell* **10**, 105-116
45. Bracha, A. L., Ramanathan, A., Huang, S., Ingber, D. E., and Schreiber, S. L. (2010) Carbon metabolism-mediated myogenic differentiation. *Nat Chem Biol* **6**, 202-204

**FOOTNOTES**

This work is supported by NIH grants AR060456 (FL), 5F32AR060674 (CMK), P41-RR00954 (JT), P60-DK20579 (JT), and P30-DK56341 (JT).

## FIGURE LEGENDS

### Figure 1 Wnt3a suppresses gene expression in ST2 cells.

(A) qPCR analyses of the effect of Wnt3a treatment on osteoblast marker gene induction in ST2 cells. (B) Total number of genes induced or suppressed (>2 fold) by Wnt3a or BMP2 after 6 or 24 hours of treatment, as detected by RNA-seq. (C) Alignment of mapped sequence reads to *Pparg* locus treated with vehicle (Control), Wnt3a or BMP2 for either 6 or 24 hours. (D) qPCR confirmation of gene suppression in response to 6 hr Wnt3a treatment. (E) qPCR analyses of the effect of *Pparg* knockdown by shRNA on osteoblast marker gene induction in ST2 cells. Two different shRNA used for *Pparg* (1 and 2); shLacZ as negative control. \*:  $p < 0.05$ ,  $n = 3$ . Error bars: SD.

### Figure 2 Wnt-induced gene suppression is independent of $\beta$ -catenin signaling.

(A, B) qPCR analyses of the effect of viral expression of dnTCF4 on gene suppression in response to Wnt3a after 6 (A) or 96 (B) hrs. (C) qPCR analyses of the effect of  $\beta$ -catenin knockdown on Wnt3a-induced gene suppression. IE: control retrovirus expressing EGFP. Two shRNA is used against  $\beta$ -catenin (shCatnbnb-A7 and -A9).

### Figure 3 Decrease in histone acetylation correlates with gene suppression.

(A-C) Western blot analyses of acid extracted histones after 6 hours Wnt3a treatment (A, C) or after 6 or 24 hours of Wnt3a or BMP2 treatment in ST2 cells (B). Acetylated H3 normalized to total H3 in A, C. Fold change  $\pm$  SD for Wnt3a over vehicle in three independent experiments in A. Coomassie staining of acid-extracted histones shown in B. Quantification shown for representative blot in C. Note different positioning of size markers from that in other blots due to the use of a gradient gel in C. (D) ChIP-seq data showing the number of genomic loci with called peaks for increased versus decreased H3K9ac, on each autosome. (E-G) ChIP-seq data showing average H3K9ac or H3K4me3 reads at the promoter regions of all (E), suppressed (F) or induced (G) genes. (H, I) H3K4me3 and/or H3K9ac profiles at the promoter region of *Pparg* (H) or *Sox5* (I), both suppressed by Wnt3a.

### Figure 4 Wnt decreases nuclear acetyl-coA and citrate levels to reduce histone acetylation.

(A-C) Effects of trichostatin A (TSA) on histone acetylation (A), gene suppression (B) and matrix mineralization (C) in response to Wnt3a. \*:  $p < 0.05$ ,  $n = 3$ . (D) HDAC or HAT activity assay performed with nuclear extracts from ST2 cells treated with vehicle or Wnt3a for 6 hours. Cells treated with TSA used as a control for HDAC activity assay. (E) Effect of Wnt3a on nuclear acetyl-coA levels. Acetyl-coA abundance is normalized to 100 ng propionyl-coA added to the nuclear extract as an internal standard. \*\*  $p = 0.004$ ,  $n = 5$ . (F) Effect of Wnt3a on nuclear citrate levels. \* $p = 0.015$ ,  $n = 6$ . CM: conditioned media. L: control L cells; Wnt3a: L cells expressing Wnt3a. Error bars: SD.

### Figure 5 Changes in acetyl-coA production affect histone acetylation and gene expression

(A) Schematic for acetyl-coA production from citrate or acetate. Acly converts citrate into acetyl-coA for histone acetylation. Acetate is converted into acetyl-coA independent of citrate. (B) Effects of sodium acetate on H3K9ac in ST2 cells treated with Wnt3a- or L-cell conditioned media (CM) for 6 hours. Propionic acid used as negative control. H3K9ac normalized to total H3. Fold change  $\pm$  SD from three independent experiments. (C-E) Effects of sodium acetate on Wnt3a-induced gene suppression at 6 hours (C), osteoblast differentiation at 72 hours (D), or matrix mineralization (E). (F-G) Effects of Acly knockdown (siAcly) on histone H3K9ac (F), or gene expression with or without Wnt3a treatment (G). siNTC: non-targeting control siRNA. Coomassie staining to show equal loading of acid-extracted histones in F. \*  $p < 0.05$ ,  $n = 3$ . Error bars: SD.

### Figure 6 Wnt suppresses glucose entry into TCA cycle.

(A-B) Graphic depiction of  $\text{CO}_2$  generation from glucose labeled with  $^{14}\text{C}$  at specific positions. Black circle denotes labeled carbon. White circle denotes unlabeled carbon. (C-F)  $^{14}\text{CO}_2$  production from [3,4-

$^{14}\text{C}_2$ ]glucose (C,D) or  $[6\text{-}^{14}\text{C}]$ glucose (E,F) in ST2 cells treated with Wnt3a or vehicle (Veh) for 24 hours. \*  $p < 0.05$   $n=5$ . Error bars: SD.

**Figure 7 Suppression of glucose metabolism reduces histone acetylation**

(A) Western blot analyses of acid extracted histones in ST2 cells cultured for 12 hours in the presence or absence of 5.5 mM glucose. Acetylated H3K9 normalized to total H3. Fold change  $\pm$  SD from three independent experiments. (B) Diagram of glucose oxidation through the TCA cycle. (C) Effect of myc-Pdk1 expression on H3K9 acetylation in ST2 cells. GFP or myc-Pdk1 was expressed from lentiviral vectors in response to Dox. GFP is a negative control. Arrow denotes myc-Pdk1; arrowhead denotes endogenous Pdk1. H3K9ac normalized to total H3. Fold change  $\pm$  SD from three independent experiments. (D) Effect of myc-Pdk1 expression on gene expression in ST2 cells infected with lentiviruses with or without Dox treatment. \*:  $p < 0.05$ ,  $n=3$ , error bar: SD.



**Table 1 shRNA sequences used in this study**

| Gene Symbol           | Insert Sequence       |
|-----------------------|-----------------------|
| LacZ                  | GCGATCGTAATCACCCGAGTG |
| RFP                   | ACAACAGCCACAACGTCTATA |
| $\beta$ -catenin – A9 | GCGTTATCAAACCCTAGCCTT |
| $\beta$ -catenin – A7 | CCATCACAGATGTTGAAACAT |
| Pparg – 1             | GCCTCCCTGATGAATAAAGAT |
| Pparg – 2             | CCTGGTTTCATTAACCTTGAT |

**Table 2 PCR primers used in this study**

| Gene Symbol | Forward                 | Reverse                   |
|-------------|-------------------------|---------------------------|
| 18s         | CGGCTACCACATCCAAGGAA    | GCTGGAATTACCGCGGCT        |
| Alpl        | CCAACCTCTTTGTGCCAGAGA   | GGCTACATTGGTGTGAGCTTTT    |
| Ibsp        | CAGAGGAGGCAAGCGTCACT    | GCTGTCTGGGTGCCAACACT      |
| Catnb1      | CCTCCCAAGTCCTTTATGAATGG | CCGTCAATATCAGCTACTTGCTCTT |
| Pparg       | GGAAAGACAACGGACAAATCAC  | TACGGATCGAAACTGGCAC       |
| Cebpa       | TGAACAAGAACAGCAACGAG    | TCACTGGTCACCTCCAGCAC      |
| Sp7         | CCCTTCTCAAGCACCAATGG    | AAGGGTGGGTAGTCATTTGCATA   |
| ID2         | ATGAAAGCCTTCAGTCCGGTG   | AGCAGACTCATCGGGTCGT       |
| Sox9        | CGGCTCCAGCAAGAACAAG     | TGCGCCACACCATGA           |
| Sox5        | TTTTCCCAACAAGCCTCACTC   | TTGCCATCGACTTCCATTGTG     |
| Lef1        | CCTACAGCGACGAGCACTTTT   | CCTTGCTTGGAGTTGACATCTG    |
| Bglap       | CAGCGGCCCTGAGTCTGA      | GCCGGAGTCTGTTCACTACCTTA   |
| Pdk1        | AGGCGTTTATCCCCCGATTC    | CGTAACCAAACCCAGCCAGG      |

Fig. 1

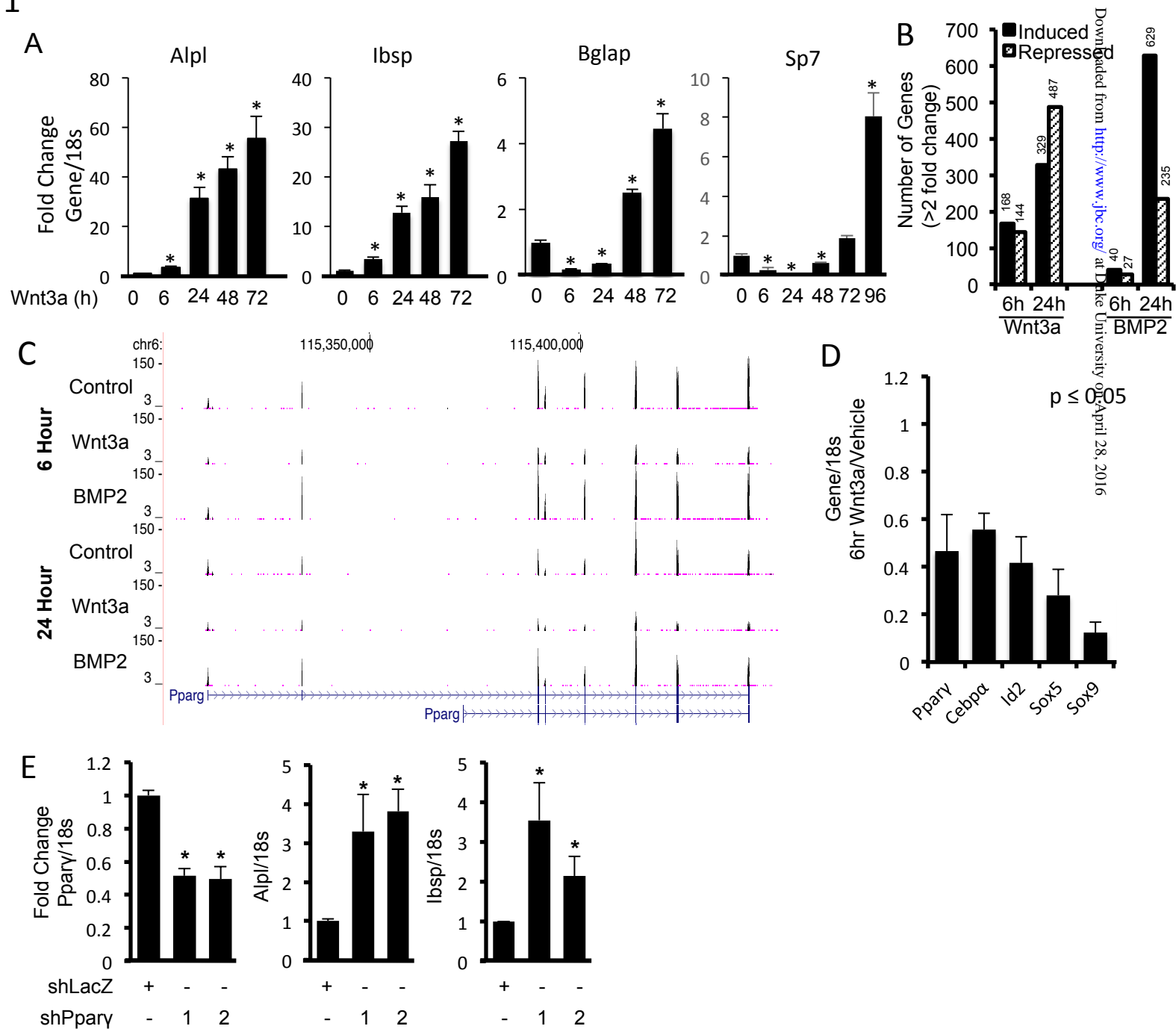
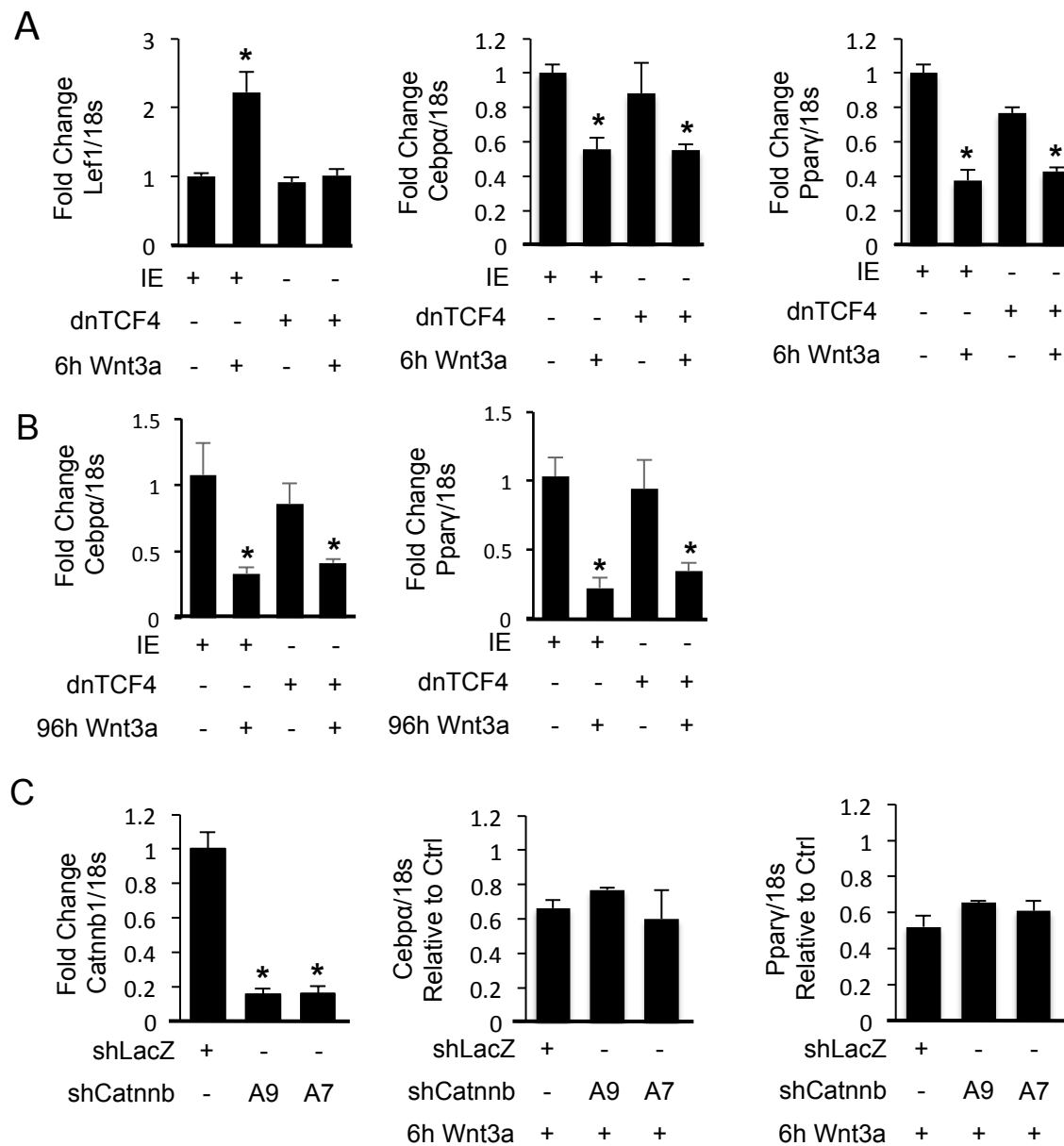


Fig. 2



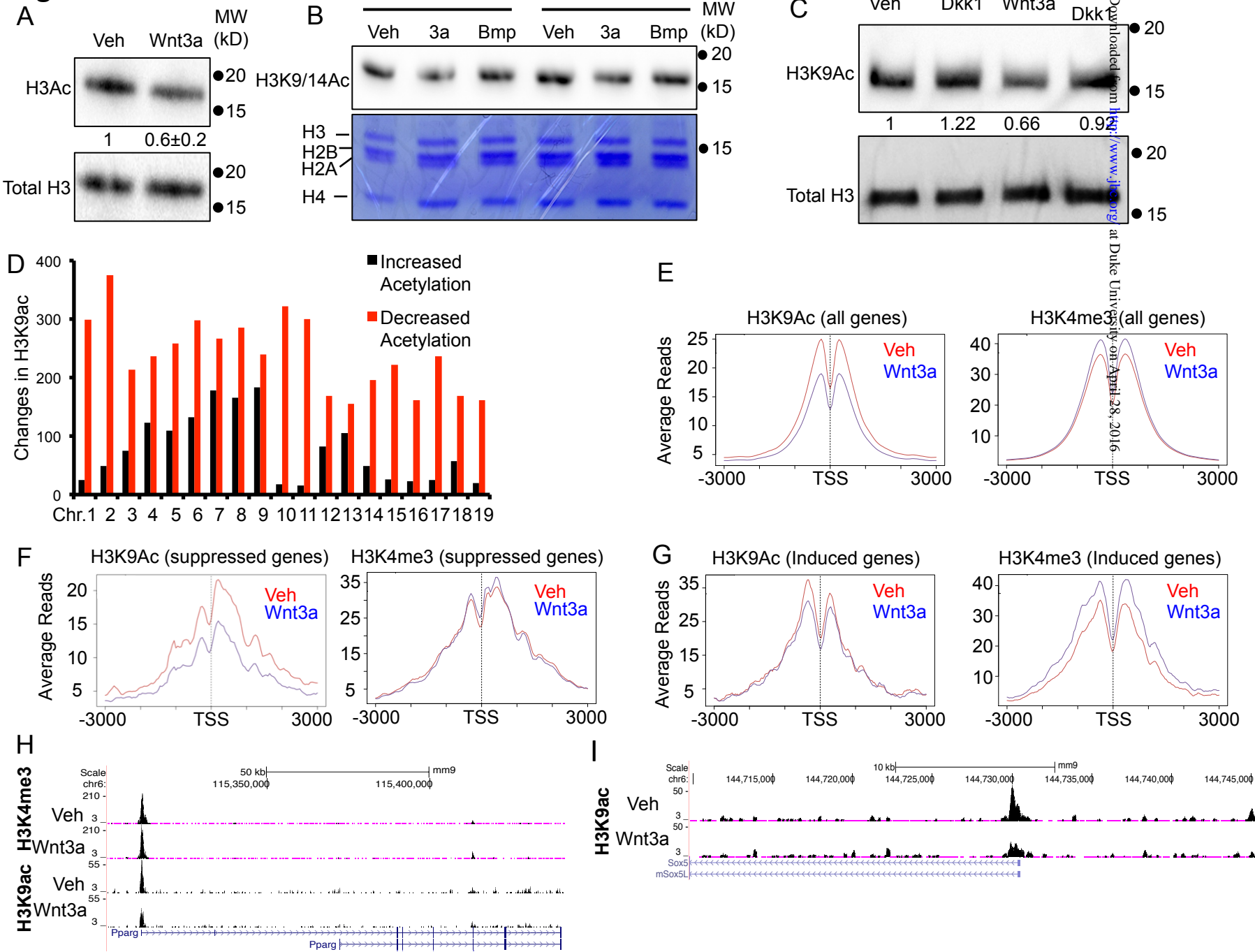
**Fig. 3**



Fig. 4

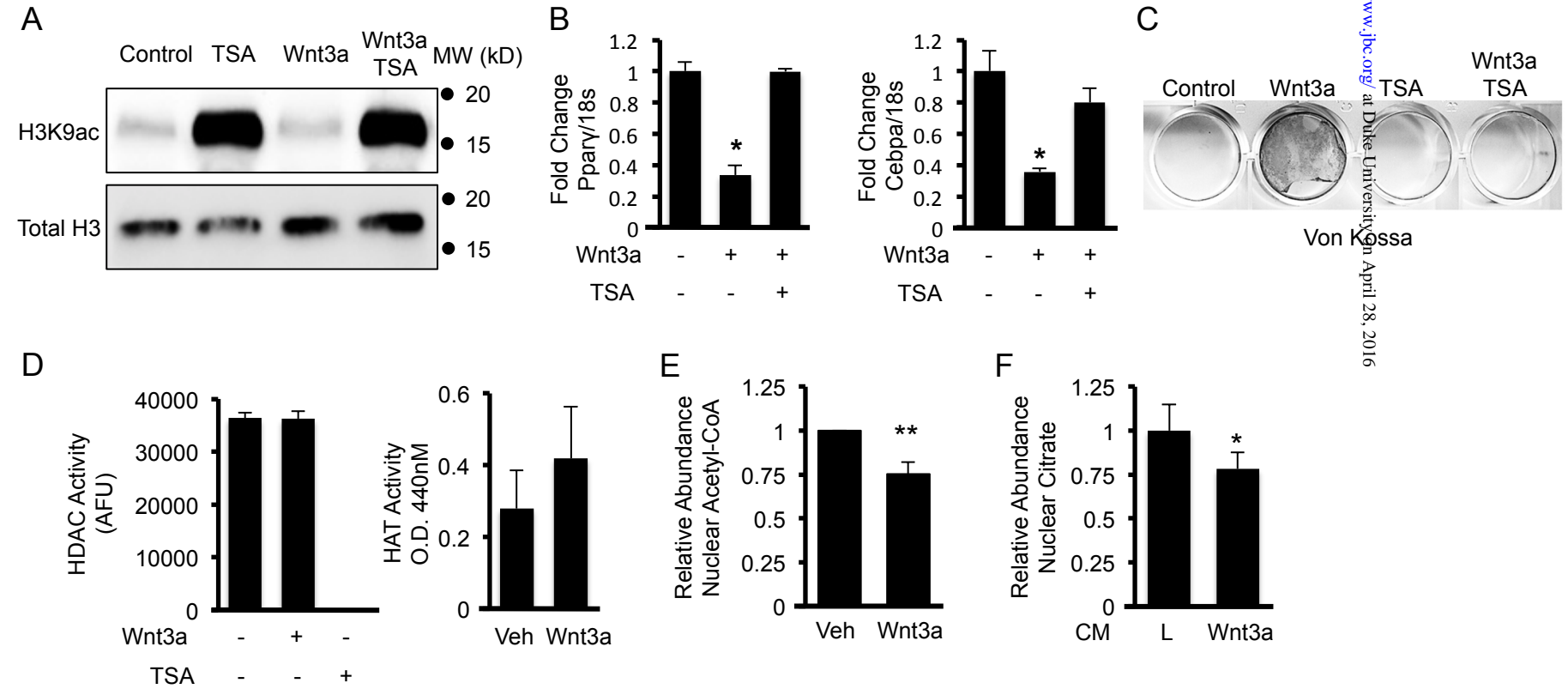


Fig. 5

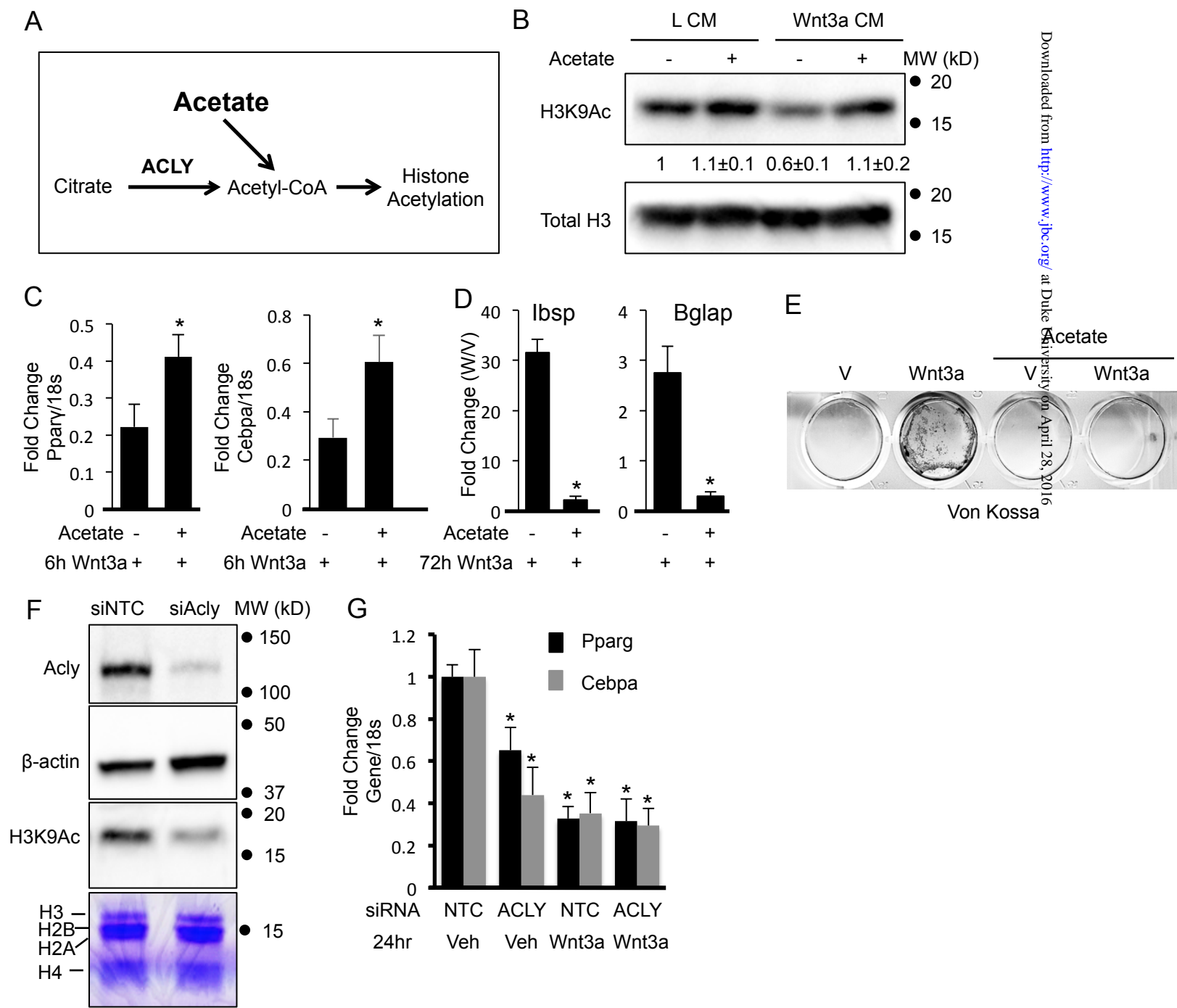


Fig. 6

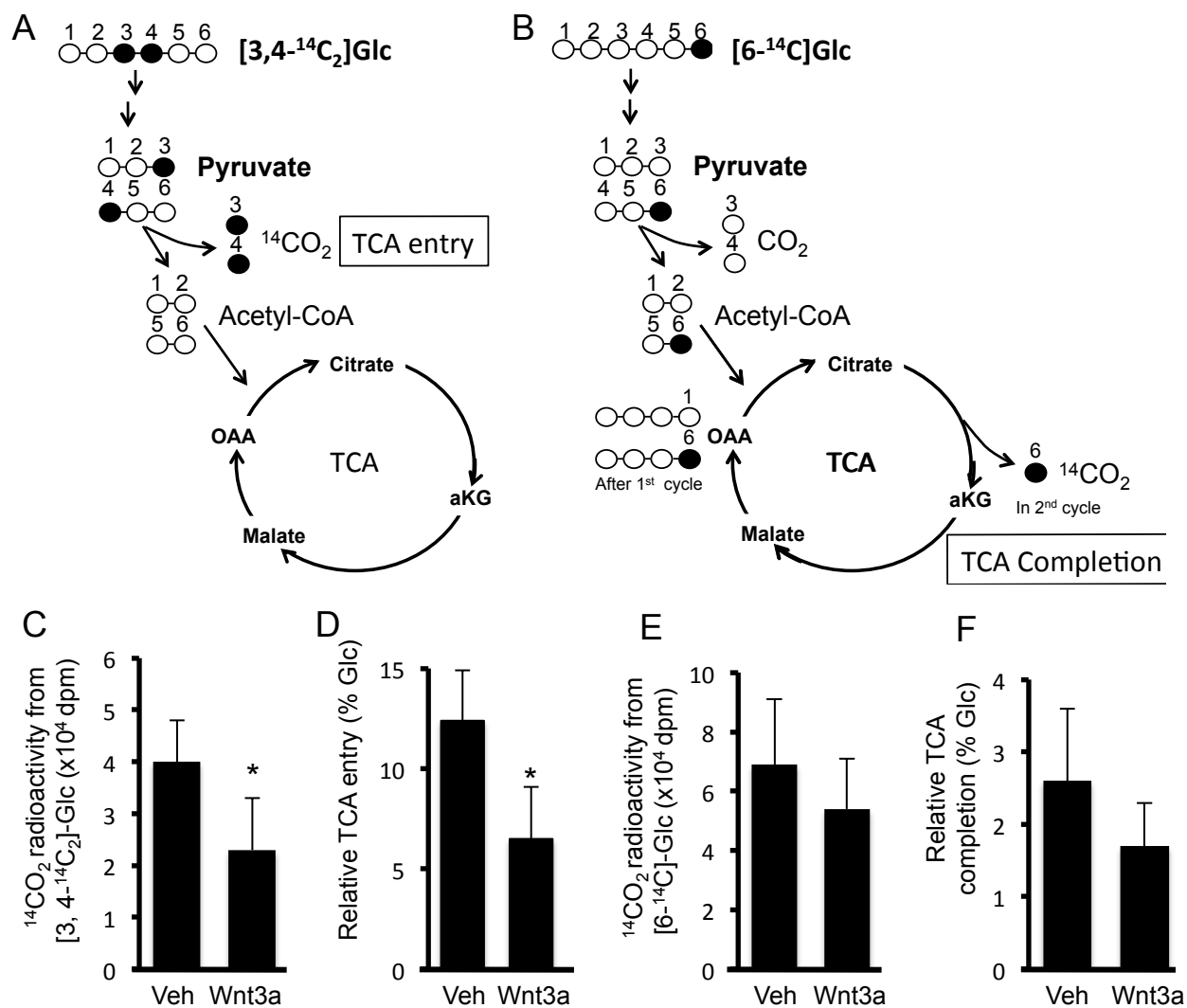
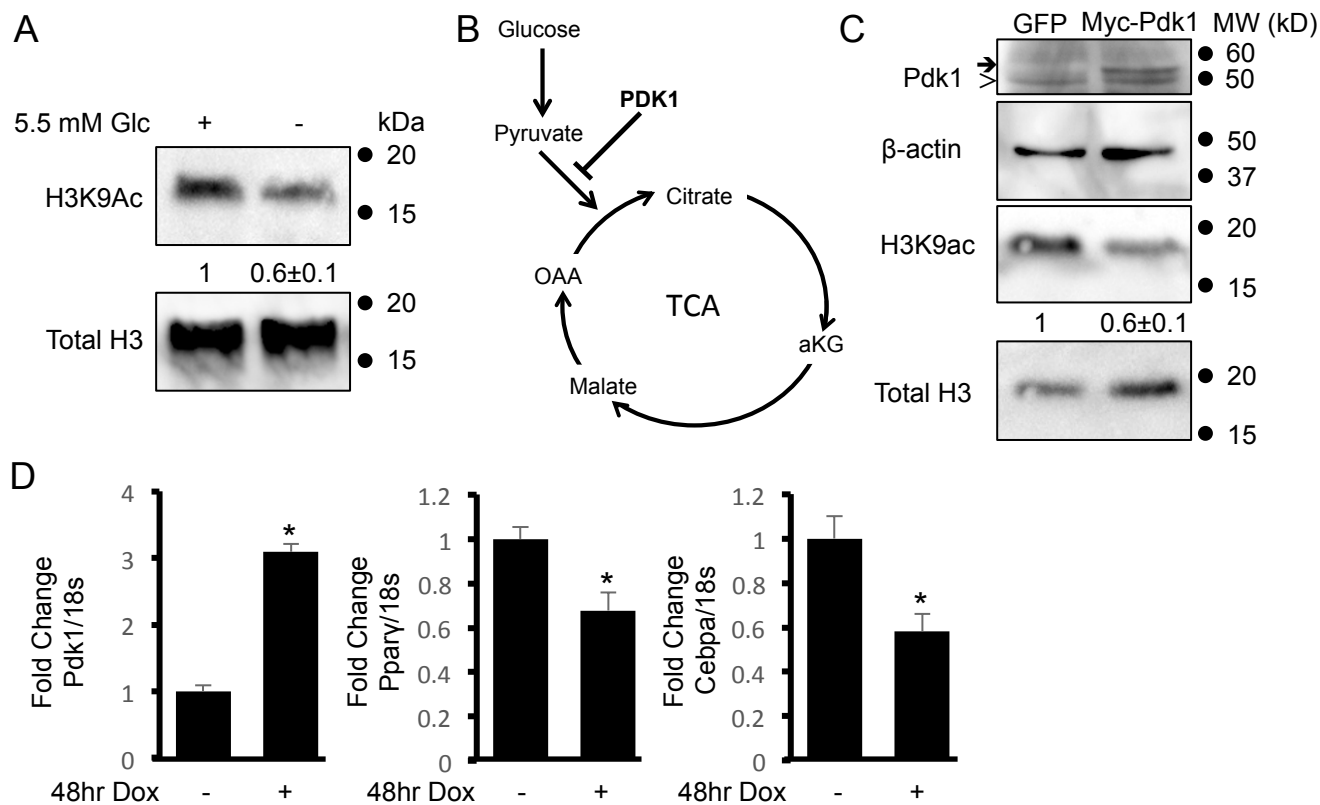


Fig. 7



**Wnt Signaling Reduces Nuclear Acetyl-coA Levels to Suppress Gene Expression  
during Osteoblast Differentiation**

Courtney M. Karner, Emel Esen, Jiakun Chen, Fong-Fu Hsu, John Turk and Fanxin Long

*J. Biol. Chem.* published online April 20, 2016

---

Access the most updated version of this article at doi: [10.1074/jbc.M115.708578](https://doi.org/10.1074/jbc.M115.708578)

Alerts:

- [When this article is cited](#)
- [When a correction for this article is posted](#)

[Click here](#) to choose from all of JBC's e-mail alerts

This article cites 0 references, 0 of which can be accessed free at  
<http://www.jbc.org/content/early/2016/04/20/jbc.M115.708578.full.html#ref-list-1>